Structure, Vibrational Spectrum, and Ring Puckering Barrier of Cyclobutane

Thomas A. Blake

William R. Wiley Environmental Molecular Sciences Laboratory, Pacific Northwest National Laboratory, P.O. Box 999, MS K8-88, Richland, Washington 99352

Sotiris S. Xantheas*

Chemical Sciences Division, Pacific Northwest National Laboratory, 902 Battelle Boulevard, P.O. Box 999, MS K1-83, Richland, Washington 99352

Received: April 21, 2006; In Final Form: July 7, 2006

We present the results of high level ab initio calculations for the structure, harmonic and anharmonic spectroscopic constants, and ring puckering barrier of cyclobutane (C_4H_8) in an effort to establish the minimum theoretical requirements needed for their accurate description. We have found that accurate estimates for the barrier between the minimum (D_{2d}) and transition state (D_{4h}) configurations require both higher levels of electron correlation [MP4, CCSD(T)] and orbital basis sets of quadruple-ζ quality or larger. By performing CCSD(T) calculations with basis sets as large as cc-pV5Z, we were able to obtain, for the first time, a value for the puckering barrier that lies within 10 cm^{-1} (or 2%) from experiment, whereas the best previously calculated values were in errors exceeding 40% of experiment. Our best estimate of 498 cm^{-1} for the puckering barrier is within 10 cm^{-1} of the experimental value proposed originally, but it lies ~50 cm^{-1} higher than the revisited value, which was obtained more recently using different assumptions regarding the coupling between the various modes. It is therefore suggested that revisiting the analysis of the experimental data might be warranted. Our best computed values (at the CCSD(T)/aug-cc-pVTZ level of theory) for the equilibrium structural parameters of C_4H_8 are $r(C-C) = 1.554$ Å, $r(C-H_\alpha) = 1.093$ Å, $r(C-H_\beta) = 1.091$ Å, $\phi(C-C-C) = 88.1°$, $\alpha(H_\alpha-C-H_\beta) = 109.15°$, and $\theta = 29.68°$ for the puckering angle. We have found that the puckering angle θ is more sensitive to the level of electron correlation than to the size of the basis set for a given method. We furthermore present anharmonic calculations that are based on a second-order perturbative evaluation of rovibrational parameters and their effects on the vibrational spectra and average structure. We have found that the anharmonic calculations predict the experimentally measured fundamental band origins within 1% ($\leq$30 cm^{-1}) for most vibrations. The results of the current study can serve as a guide for future calculations on the substituted four-member ring hydrocarbon compounds. To this end we present a method for estimating the puckering barrier height at higher levels of electron correlation [MP4, CCSD(T)] from the MP2 results that can be used in chemically similar compounds.

I. Introduction

Cyclobutane (C_4H_8) represents the prototype for investigating the interplay between angle and torsional strain and the molecular structure and spectra for substituted four-member ring hydrocarbons.[1,2] The analysis of the infrared (IR) spectra of cyclobutane is more tractable than for its substituted analogues such as C_4Cl_8, $C_4(OH)_8$, and C_4F_8, which have smaller rotational constants and higher density of rovibrational-puckering states, a fact that makes the analysis of their IR spectra more difficult. The equilibrium structure of these molecular systems can be thought of oscillating between two equivalent puckered equilibrium structures through a transition state following a large amplitude, low-frequency mode. This double-well potential results in a splitting of the low-frequency puckering energy levels, a fact that imposes a distinctive sideband structure to the molecule's fundamental vibrational transitions.

The ν_6 (b_{2u}) ring puckering mode of C_4H_8 at 198 cm^{-1} is not IR active and is only weakly Raman active, but it results in a series of combination hot bands that are associated with the fundamental bands. This sideband structure arises from transitions from either the ground-state ring puckering levels $0\pm$ or from excited ring puckering levels $n\pm$ that may be populated. The height of the puckering barrier [energy difference between its minimum (D_{2d}) and transition state (D_{4h}) configurations] has been previously experimentally estimated from the analysis of the puckering sideband structure of the higher frequency IR fundamental bands. The analysis is performed by assuming an even-order polynomial[3,4] in the puckering coordinate q (typically a quadratic−quartic one), making several assumptions regarding the reduced mass, and taking into account the caveat that the relationship between q and a geometrical coordinate is obscured due to the fact that they are related by a nonlinear transformation.[3] Some of the outstanding issues associated with the fitting of the sideband spectra in order to obtain the puckering barrier can be summarized as follows: (i) truncation of the even-order polynomial used to describe the puckering potential, (ii) coordinate dependence of the reduced mass, and (iii) coupling with other vibrational modes.

Ueda and Shimanouchi[5] first obtained a puckering barrier of 448.1 ± 18 cm^{-1} and a dihedral angle of 34° for the C_4 ring by analyzing the sidebands on the low wavenumber side of the

* Corresponding author. Phone: 509-375-3684. Fax: 509-375-4381. E-mail: sotiris.xantheas@pnl.gov.

10.1021/jp062472r CCC: $33.50
Published on Web 08/17/2006

ν_{18} (e_g) CH_2 symmetric stretch mode at 2878 cm^{-1} with a quadratic−quartic potential. Stone and Mills[6] subsequently reanalyzed the spectra of the ν_{18} band showing that the sideband transitions were spread out over 100 cm^{-1} to the red of the band origin. By using a quadratic−quartic potential and assuming the separability of the ring puckering coordinate from the rest of the vibrational coordinates and constant reduced mass, they also analyzed the sideband structure of the ν_{14} (b_{1g}) CH_2-scissoring mode at 1453 cm^{-1} and obtained a puckering barrier of 503 cm^{-1} and a dihedral angle of 35°. Furthermore, they pointed out that other vibrational modes of b_{1g} and e_g symmetry should exhibit a similar sideband structure. However, because these bands are weak, it was not possible to assign ring-puckering sideband structure to any other IR active fundamentals. Miller and Capwell[7] also assumed a constant reduced mass and a quadratic−quartic polynomial and using additional Raman data obtained a puckering barrier of 518 ± 5 cm^{-1}. The effect of the coordinate dependence of the reduced mass in the Hamiltonian used to fit the spectra was examined by Malloy and Lafferty,[8] who performed a least-squares fit of all previous data. They found that there is an isotopic dependence of ∼14 cm^{-1} in the barrier in C_4H_8 and C_4D_8, indicating that the H/D atoms participate in the puckering coordinate. This proposition is also supported by the fact that higher order kinetic energy effects result in a shift of just ∼3 cm^{-1} in the barrier height and therefore cannot fully account for the isotopic effect, which must come from the coupling with other vibrational modes. The mixing of the CH_2-scissoring and CH_2-rocking with the ring-puckering motion introduced substantial uncertainty in the range of dihedral angles (28.9−37°) and yielded a range of 513.2−515.6 cm^{-1} for the puckering barrier. They suggested that a multidimensional treatment of the puckering motion would be more appropriate.

The importance of obtaining a more accurate value for the dihedral angle prompted an electron diffraction study by Egawa et al.,[9] the results of which were analyzed conjointly with the FTIR spectra of the ν_{14} (CH_2-scissoring) and ν_{16} (CH_2-rocking) bands. This analysis produced r_z(C−C) = 1.552 ± 0.001 Å, r_z(C−H) = 1.093 ± 0.003 Å, α_z(H−C−H) = 106.4 ± 1.3°, and a ring dihedral angle of 27.9 ± 1.6°, while the r_g distances of the C−C and C−H bonds were 1.554 ± 0.001 Å and 1.109 ± 0.003 Å, respectively. In this notation, subscript "z" denotes the average structure associated with the average configuration of the atoms for a specific vibrational state evaluated by a partial correction for the effects of vibration, whereas subscript "g" indicates bond distances (center of gravity of the probability distribution function) obtained from electron diffraction.[10] The latter can be related to the former with only the knowledge of the harmonic force constants.[11] It should be noted that the electron diffraction data were analyzed following the assumption based on an earlier ab initio study[12] that the axial and equatorial C−H stretches differ by <0.001 Å, a difference that the electron diffraction intensity is insensitive to. By including up to a sixth-order term in the double-well potential and assuming a linear coupling of the puckering mode with only the CH_2-rocking mode and a coordinate-dependent reduced mass, they produced an equilibrium dihedral angle of 28.8 ± 1.1° and a vibrationally averaged value of 27.5 ± 1.1° in good agreement with the result from the electron diffraction study. Furthermore, their estimate for the barrier was 510 ± 3 cm^{-1}. In a subsequent study, Egawa et al.[13] recorded the IR spectrum of the ν_{16} (a_{2u}) CH_2-rocking band at 626 cm^{-1} at a higher resolution and used a one-dimensional potential up to sixth order with linear coupling of the puckering coordinate with the b_{2u} CH_2-rocking mode to obtain values of 649 ± 11 cm^{-1} for the puckering barrier and 31.4 ± 1.3° for the dihedral angle. These values are quite different than the ones obtained from their previous analysis of the sideband structure of the ν_{14} and ν_{16} bands, and the difference was ascribed to higher order mixing between the ν_6 and ν_{16} bands. They subsequently used a two-dimensional potential to analyze this mixing, which produced a significantly lower barrier height of 449 ± 9 cm^{-1} and a dihedral angle of 27.8 ± 1.2°.

In contrast to the previous plethora of experimental studies, there has been only a handful of mainly low-level ab initio calculations on the puckering barrier of C_4H_8. Champion et al.[14] used the semirigid bender method to fit the vibrational frequencies on a puckering vibration path obtained from HF/4-31G** calculations, a level of theory that predicts a puckering barrier of 331 cm^{-1}. Fischer et al.[15] reported barriers of 318 cm^{-1} at the HF/6-31G* and 792 cm^{-1} at the MP2/6-31G* levels of theory, respectively. A more recent study by Henseler and Hohneicher[16] at the HF, density functional (B3LYP), and MP2 levels of theory with a variety of basis sets ranging from minimal (STO-3G) to split valence including polarization and diffuse functions [6-31G(d), 6-31G(d,p), 6-31G(2d,p) and 6-31++G-(d,p)] produced barriers that are either too low by about 200 cm^{-1} (HF, B3LYP) or too high by about 400 cm^{-1} (MP2) when compared to the experimental estimates. Furthermore, the barrier was found to increase with basis set for all three levels of theory considered in that study for the range of basis sets examined. It should be noted, however, that all previous calculations were performed with basis sets of at best double-ζ quality.

The absence of high-level ab initio calculations on the structure and puckering barrier of C_4H_8 is quite surprising given that the analysis of the experimental data produced a range of ∼100 cm^{-1} for the puckering barrier and ∼10° for the dihedral angle. Furthermore, all models used to fit the experimental data rely on structural information from electron diffraction experiments the analysis of which was based on the results of low level ab initio calculations, especially on the assumption that the axial and equatorial C−H bonds lengths are within 0.001 Å, i.e., below the detection limit of the electron diffraction experiment. The previous discussion suggests that high level ab initio calculations on this system are warranted in order to derive more accurate structural and energetic information. In particular, it is of interest to establish the minimum theoretical requirements as regards both level of theory and basis set for the accurate description of the puckering barrier as these can serve as starting points for subsequent calculations on substituted analogues of cyclobutane. In section II, we outline the details of the ab initio calculations. In section III we present the results for the optimal geometry, harmonic and anharmonic vibrational spectra, spectroscopic constants, and the puckering barrier of C_4H_8. Final conclusions are summarized in section IV.

II. Theoretical Approach

We obtained optimal geometries for the D_{2d} (minimum) and D_{4h} (transition state) structures, shown in Figure 1, by full geometry optimizations at the Hartree−Fock (HF), the second- and fourth-order Moller−Plesset (MP2, MP4), and the coupled-cluster singles and doubles with perturbative estimate of triple excitations [CCSD(T)] levels of theory using the family of plain and augmented correlation consistent basis sets, cc-pV*n*Z and aug-cc-pV*n*Z (n = D, T, Q, 5).[17] Only the valence electrons were correlated. The geometry optimizations at the HF and MP2 levels of theory with the cc-pVDZ (aug-cc-pVDZ), cc-pVTZ (aug-cc-pVTZ), and cc-pVQZ basis sets were performed using

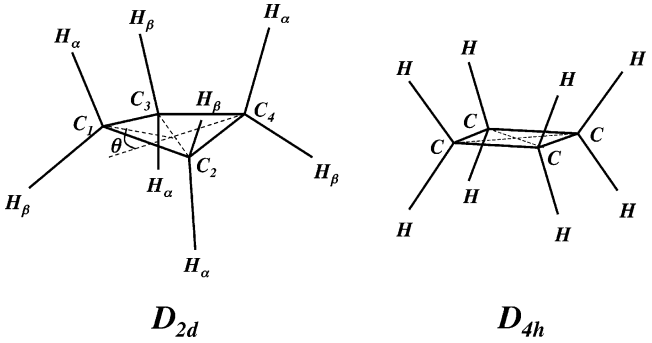

Figure 1. Conformations of the minimum (D_{2d}) and transition state (D_{4h}) geometries of C_4H_8 and definition of the puckering angle θ.

analytic first derivatives. Geometry optimizations at the MP4 and CCSD(T) levels of theory with the cc-pVDZ (aug-cc-pVDZ) and cc-pVTZ (aug-cc-pVTZ) basis sets were carried out numerically using a *Z*-matrix description of the molecular geometry in terms of the six (for D_{2d} symmetry) and three (for D_{4h} symmetry) unique internal coordinates. In all geometry optimizations (using both analytical and numerical first derivatives), the geometries of the stationary points (minimum, transition state) were converged to an accuracy in the corresponding energy of $<5 \times 10^{-7}$ hartree (<0.1 cm^{-1}). Single point calculations at the best optimal geometries for each level of theory were performed with the larger basis sets. The largest MP2 calculation was performed with the aug-cc-pV5Z basis set consisting of the segmented contractions [6s5p4d3f2g1h]+(1s1p1d1f1g1h) for the carbon and hydrogen atoms for a total of 1148 contracted Gaussian basis functions. The largest CCSD(T) calculation was performed with the cc-pV5Z basis set having a total of 804 contracted Gaussian functions. Anharmonic frequencies[18] and anharmonic vibrational−rotational couplings[19] were computed by numerical differentiation along normal modes at the MP2 level of theory. The calculations were carried out using the Gaussian 98 and 03 (ref 20), MOLPRO (ref 21), and NWChem (ref 22) suites of codes at the Molecular Science Computing Facility (MSCF) in the Environmental Molecular Sciences Laboratory at Pacific Northwest National Laboratory and at the National Energy Research Scientific Computing Center (NERSC) at Lawrence Berkeley National Laboratory.

III. Results and Discussion

a. Optimal Geometry. The optimal internal coordinates of the geometries of the minimum (D_{2d}) and the transition state (D_{4h}) at the various levels of theory and basis sets considered in this study are listed in Table 1. The labeling of the atoms is shown in Figure 1. The definition of the angles is consistent with the one adapted in the electron diffraction study;[9] viz., α is the ($H_\alpha-C-H_\beta$) angle and θ is the puckering angle defined as $\theta = 180° - \tau(C_1C_2C_3C_4)$, where $\tau(C_1C_2C_3C_4)$ is the torsional angle[23] between the planes determined by atoms C_1, C_2, C_3 and C_2, C_3, C_4, respectively, and the numbering of the carbon atoms is shown in Figure 1. The higher symmetry of the transition state (D_{4h}) implies that $r(C-H_\alpha) = r(C-H_\beta)$, $\phi(C-C-C) = 90°$, and $\theta = 0°$, resulting in only three unique internal coordinates that fully specify the geometry under this symmetry.

From Table 1 it is seen that for the minimum (D_{2d}) geometry the difference between the two sets of C−H bond lengths [$r(C-H_\alpha)$ and $r(C-H_\beta)$] is indeed small; for some of the higher correlation methods [MP4, CCSD(T)] the difference is ∼0.002 Å, a value that is still below the sensitivity for electron diffraction. As a general trend, the use of larger basis sets (i.e. going from cc-pVDZ to cc-pVQZ) tends to decrease both C−H and C−C bond lengths, whereas within a fixed basis set the higher correlation methods [i.e., going from MP2 to MP4 and CCSD(T)] have an opposite effect, increasing both bond lengths. The best computed values for the C−H bond lengths are $r(C-H_\alpha) = 1.092$ Å, $r(C-H_\beta) = 1.090$ Å at both MP4 and CCSD(T) levels of theory. The computed value for $r(C-H_\alpha)$ is within the experimental error bar of the one obtained from electron diffraction experiment,[9] viz., 1.092 ± 0.001 Å. Similarly, the best computed value for the C−C bond length is 1.552 Å, identical with the one obtained from the analysis of the electron diffraction data. It should again be noted that the experimentally reported structures for the bond lengths correspond to average structures, which are evaluated by a partial correction for the effect of vibration (r_z). The effects of vibrational averaging on the structure will be discussed later in this section.

The ϕ(C−C−C) and α(H−C−H) angles are both almost insensitive to the basis set and level of electron correlation; all combinations of theoretical methods and basis sets used in this study produce results that are within <1° of each other for both of these angles. The computed α(H−C−H) angles are ∼3° larger than the value obtained from electron diffraction[9] and lie outside the error bar assigned to the experimental average structure. The puckering angle θ does, however, exhibit sensitivity mostly to the level of electron correlation rather than to the basis set within a fixed level of theory. Whereas the optimal value is 26.33° at the HF level with the cc-pVQZ set, higher levels of electron correlation produce significantly larger values. The puckering angle decreases somewhat with increases in both the basis set size as well as the level of electron correlation. The best computed value for the puckering angle at the CCSD(T)/aug-cc-pVTZ level of theory is 29.68°, a value that, although on the high side, is within the error bar of the experimentally determined[9] equilibrium value of $\theta_e = 28.8 \pm 1.1°$. We also note that the range of dihedral values that are determined on the basis of fits of the spectra has drifted down from 35° to 29° with time, in steps that were always larger than the error bars of the earlier result. Overall the results of Table 1 indicate that the geometry of the minimum is converged with the triple-ζ quality set as there are minimal changes (<0.001 Å for the C−H bonds, <0.002 for the C−C bonds and <0.2° for the bond angles) upon reoptimization with the larger cc-pVQZ set and that the computed bond lengths and angles are very close to the experimentally obtained results.

The effects of vibrational averaging on the minimum energy structure and spectroscopic constants at the MP2 level of theory are shown in Table 2 where they are compared to available experimental data.[9,24] In this Table subscript "e" denotes the equilibrium whereas "z" the vibrationally averaged values. The effect of basis set is also examined by comparing the results with the aug-cc-pVDZ and cc-pVTZ sets. In general, there is good agreement between the calculated and measured spectroscopic constants. The quartic vibrationally averaged centrifugal distortion constants D_J, D_{JK}, and D_K of Table 2 are computed in the symmetrically reduced Watson Hamiltonian. The effect of vibrational averaging on the bond lengths and bend angles is as follows: $\Delta r_{0-e}(C-H_\alpha) = \Delta r_{0-e}(C-H_\beta) = 0.006$ Å, $\Delta r_{0-e}(C-C) = 0.009$ Å, $\Delta\phi_{0-e}(C-C-C) = 0.12°$, $\Delta\alpha_{0-e}(H_\alpha-C-H_\beta) = -0.25°$, $\Delta\theta_{0-e} = -0.85°$, where the difference is taken with respect to the equilibrium geometry ("e"). We observe typical bond length elongations of 0.006−0.009 Å, CCC skeletal bend angle increases of 0.12°, and covalent bend angle decreases of 0.25°. The largest effect was found for the dihedral angle, θ, which decreases by about 1°

TABLE 1: Optimal Internal Coordinates of the (D_{2d}) Minimum and the (D_{4h}) Transition State of C_4H_8 at Various Levels of Theory

D_{2d} minimum							
level of theory	basis set	r(C−H$_\alpha$), Å	r(C−H$_\beta$), Å	r(C−C), Å	ϕ(C−C−C), deg	α(H$_\alpha$−C−H$_\beta$), deg	θ, deg[a]
HF	cc-pVDZ	1.0922	1.0911	1.5459	88.46	108.41	26.48
	cc-pVTZ	1.0832	1.0819	1.5438	88.47	108.52	26.38
	cc-pVQZ	1.0827	1.0814	1.5434	88.48	108.52	26.33
MP2	cc-pVDZ	1.1034	1.1020	1.5530	87.72	109.03	32.12
	cc-pVTZ	1.0892	1.0875	1.5454	87.76	109.21	31.87
	cc-pVQZ	1.0882	1.0866	1.5428	87.81	109.17	31.51
	aug-cc-pVDZ	1.1016	1.1002	1.5573	87.81	109.25	31.51
	aug-cc-pVTZ	1.0900	1.0883	1.5463	87.79	109.25	31.66
MP4	cc-pVDZ	1.1066	1.1050	1.5596	87.88	108.95	30.99
	cc-pVTZ	1.0921	1.0902	1.5522	87.94	109.14	30.58
	aug-cc-pVDZ	1.1051	1.1035	1.5648	87.98	109.17	30.24
	aug-cc-pVTZ	1.0930	1.0911	1.5533	87.98	109.17	30.22
CCSD(T)	cc-pVDZ	1.1069	1.1053	1.5606	87.93	108.95	30.60
	cc-pVTZ	1.0920	1.0901	1.5524	88.00	109.13	30.11
	aug-cc-pVDZ	1.1054	1.1037	1.5656	88.04	109.17	29.82
	aug-cc-pVTZ	1.0929	1.0910	1.5535	88.06	109.15	29.68
exp[b]		1.093 ± 0.001[c]		1.552 ± 0.001[c]		106.4 ± 1.3[c]	28.8 ±1.1[d]

D_{4h} transition state				
level of theory	basis set	r(C−H$_\alpha$), Å	r(C−C), Å	α(H$_\alpha$−C−H$_\beta$), deg
HF	cc-pVDZ	1.0910	1.5498	107.86
	cc-pVTZ	1.0820	1.5478	107.96
	cc-pVQZ	1.0814	1.5474	107.96
MP2	cc-pVDZ	1.1018	1.5585	108.07
	cc-pVTZ	1.0873	1.5509	108.23
	cc-pVQZ	1.0863	1.5482	108.22
	aug-cc-pVDZ	1.1000	1.5628	108.31
	aug-cc-pVTZ	1.0881	1.5519	108.33
MP4	cc-pVDZ	1.1049	1.5647	108.09
	cc-pVTZ	1.0903	1.5572	108.26
	aug-cc-pVDZ	1.1036	1.5699	108.33
	aug-cc-pVTZ	1.0911	1.5585	108.37
CCSD(T)	cc-pVDZ	1.1053	1.5656	108.12
	cc-pVTZ	1.0903	1.5574	108.28
	aug-cc-pVDZ	1.1039	1.5705	108.35
	aug-cc-pVTZ	1.0911	1.5585	108.37

[a] The puckering angle is $\theta = 180° - \tau(C_1C_2C_3C_4)$; see the text and Figure 1. [b] Reference 9. [c] Average structure (r_z). [d] Equilibrium structure (θ_e).

upon vibrational averaging. The angle β in Table 2 is defined as the angle between the bisectors of the H−C−H and C−C−C angles. The ratio $\delta = \beta/\theta$ can be obtained from the analysis of the experimental data.[9] Our calculated value of 0.19 for the vibrationally averaged MP2/cc-pVTZ geometry agrees very well with the experimentally estimated ratio of 0.22 for this quantity.

With regard to the geometry of the transition state (D_{4h}), the C−H bond distance is almost identical (within <0.0002 Å) to the shorter [r(C−H$_\beta$)] of the two C−H bond distances at the minimum, whereas the C−C bond length is ∼0.004 Å longer than the corresponding value at the minimum. The elongation of the C−C bond length at the transition state with respect to the minimum configuration can be attributed to the additional ring strain at the D_{4h} geometry, an effect that is reduced at the minimum geometry due to the puckering of the C_4 ring. The H−C−H angle is ∼1° smaller than the one at the minimum. Finally, the imaginary harmonic vibrational frequency at the D_{4h} transition state configuration at the MP2 level of theory with various basis sets used in this study is 179 cm^{-1} (cc-pVDZ), 190 cm^{-1} (cc-pVTZ), 208 cm^{-1} (aug-cc-pVDZ), and 180 cm^{-1} (aug-cc-pVTZ).

b. Ring-Puckering Barrier. The energies of the minimum (D_{2d}) and transition state (D_{4h}) configurations (in au) and the puckering barrier ΔE_e (in cm^{-1}) are listed in Table 3. The variation of the barrier height with basis set for the various levels

TABLE 2: Effect of Vibrational Averaging[a] on the Spectroscopic and Structural Constants of Cyclobutane and Comparison with Experimental Values for the Ground State

constants[b]	MP2/aug-cc-pVDZ	MP2/cc-pVTZ	experiment
$A_z = B_z$ (cm^{-1})	0.34982	0.35597	0.35582[c]
$A_e = B_e$ (cm^{-1})	0.35388	0.35999	
C_z (cm^{-1})	0.20940	0.21302	
C_e (cm^{-1})	0.21233	0.21599	
D_J (cm^{-1})	1.8206×10^{-7}	1.9028×10^{-7}	1.88×10^{-7} [c]
D_{JK} (cm^{-1})	-2.2993×10^{-7}	-2.4077×10^{-7}	2.3×10^{-7} [c]
D_K (cm^{-1})	1.1128×10^{-7}	1.1748×10^{-7}	
ZPE (harmonic), cm^{-1}	24406.1	24601.7	
ZPE (fundamental),cm^{-1}	23597.3	23817.2	
ZPE (anharmonic),cm^{-1}	24075.0	24275.2	
r_z(C−C), Å	1.566	1.554	1.552[d]
r_z(C−H), Å	1.106, 1.108	1.093, 1.095	1.093[d]
α_z(H−C−H), deg	109.00	109.03	106.4[d]
θ_z(dihedral), deg	30.66	30.90	27.9[d]
β_z, deg	5.86	5.91	6.2[d]
$\delta = \beta/\theta$	0.19	0.19	0.22[d]

[a] Estimated at the MP2 level of theory with the aug-cc-pVDZ and cc-pVTZ basis sets. [b] Subscripts "e" and "z" denote equilibrium and vibrationally averaged quantities, respectively, and the D_J, D_{JK}, and D_K constants correspond to the vibrationally averaged geometry. [c] Reference 24. [d] Reference 9.

TABLE 3: Energies of the (D_{2d}) Minimum and the (D_{4h}) Transition State (au) and Their Energy Separation (cm^{-1}) at Various Levels of Theory

level of theory	basis set	geometry	E (D_{2d}), au	E (D_{4h}), au	ΔE_e, cm^{-1} [a]
HF	cc-pVDZ	optimized	−156.107 431 9	−156.105 788 2	**360.7**
	cc-pVTZ	optimized	−156.150 607 7	−156.148 947 5	**364.3**
	cc-pVQZ	optimized	−156.160 384 8	−156.158 743 2	**360.3**
	cc-pV5Z	cc-pVQZ	−156.162 748 8	−156.161 117 2	**358.1**
MP2	cc-pVDZ	optimized	−156.676 926 1	−156.673 114 7	**836.5**
	cc-pVTZ	optimized	−156.842 538 0	−156.838 795 2	**821.4**
	cc-pVQZ	cc-pVTZ	−156.894 203 7	−156.890 859 3	734.0
		optimized	−156.894 224 0	−156.890 878 8	**734.2**
	cc-pV5Z	cc-pVTZ	−156.912 369 7	−156.909 157 1	705.1
		cc-pVQZ	−156.912 399 3	−156.909 185 7	**705.3**
	CBS				**691**[b]
	aug-cc-pVDZ	optimized	−156.702 353 2	−156.698 358 8	**876.6**
	aug-cc-pVTZ	optimized	−156.853 056 0	−156.849 611 4	**756.0**
	aug-cc-pVQZ	aug-cc-pVTZ	−156.898 897 9	−156.895 653 5	**712.0**
	aug-cc-pV5Z	aug-cc-pVTZ	−156.914 624 5	−156.911 451 3	**696.4**
	CBS				**687**[b]
MP4	cc-pVDZ	optimized	−156.747 166 6	−156.743 942 4	**707.0**
	cc-pVTZ	optimized	−156.914 211 8	−156.911 102 2	**682.4**
	cc-pVQZ	cc-pVTZ	−156.960 583 0	−156.957 913 6	**585.9**
	CBS				**543**[c]
	aug-cc-pVDZ	optimized	−156.775 239 1	−156.771 890 7	**734.9**
	aug-cc-pVTZ	optimized	−156.924 828 5	−156.922 071 1	**605.2**
	aug-cc-pVQZ	aug-cc-pVTZ	−156.964 408 9	−156.961 852 4	**561.1**
	CBS				**538**,[b] **536**[c]
CCSD(T)	cc-pVDZ	optimized	−156.748 833 4	−156.745 806 1	**664.4**
	cc-pVTZ	optimized	−156.913 623 1	−156.910 703 5	**640.8**
	cc-pVQZ	cc-pVTZ	−156.959 551 1	−156.957 066 9	**545.2**
	cc-pV5Z	cc-pVTZ	−156.973 263 5	−156.090 865	**516.8**
	CBS				**505**,[b] **503**[c]
	aug-cc-pVDZ	optimized	−156.776 451 3	−156.773 292 6	**693.2**
	aug-cc-pVTZ	optimized	−156.924 171 8	−156.921 601 1	**564.2**
	aug-cc-pVQZ	aug-cc-pVTZ	−156.963 363 8	−156.960 992 6	**520.4**
	CBS				**498**,[b] **495**[c]

[a] Bold entries denote the best estimate for the puckering barrier (ΔE_e) at the corresponding level of theory and basis set. [b] Based on an exponential extrapolation, method a (see the text). [c] Based on the difference with the MP2 results, method b (see the text).

of theory considered here is shown in Figure 2. In this figure, the *x*-axis corresponds to the cardinal number of the basis sets (n = 2, 3, 4, 5 for DZ, TZ, QZ and 5Z, respectively). Open symbols with solid lines trace the results with the family of plain sets (cc-pV*n*Z), whereas filled symbols with dotted lines trace the ones with the family of augmented (aug-cc-pV*n*Z) basis sets. The MP2 (MP4) results are denoted by circles (squares), while the CCSD(T) results are indicated by triangles.

To arrive at an accurate estimate for the barrier height, we have systematically examined the effect of the following three factors on the relative energetics of the minimum and transition state configurations: (i) the level of electron correlation, (ii) the size of the orbital basis set, and (iii) the optimal geometry.

The effect of electron correlation on this conformational change is examined at the MP2, MP4, and CCSD(T) levels of theory. The family of correlation-consistent basis sets provides a vehicle for arriving at the complete basis set (CBS) limits for these methods. The effect of the optimal geometry on the barrier is investigated by performing single point energy calculations for the minimum and the transition state with larger basis sets at the optimal geometries obtained with smaller basis sets. For instance, single point MP2/cc-pVQZ calculations at the MP2/cc-pVTZ-optimized geometries produced a barrier of 734.0 cm^{-1}, only 0.2 cm^{-1} different than the one obtained upon reoptimization of the geometries with the cc-pVQZ basis set (734.2 cm^{-1}). The same difference in the barrier (0.2 cm^{-1}) was obtained upon performing single point MP2 calculations with the larger cc-pV5Z set at the cc-pVTZ and cc-pVQZ optimal geometries, respectively. In this case, however, the use of the larger set (cc-pV5Z) had by far a bigger effect on the

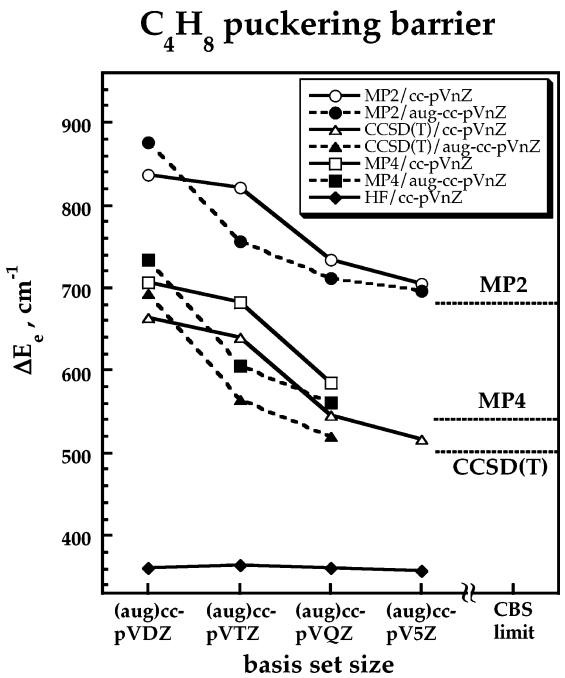

Figure 2. Variation of the puckering barrier (in cm^{-1}) with basis set at various levels of theory. The *x*-axis corresponds to the cardinal number of the cc basis sets (n = 2, 3, 4, 5 for DZ, TZ, QZ and 5Z, respectively). Open symbols/solid lines trace the results with the plain sets (cc-pV*n*Z), whereas filled symbols/broken lines denote the ones with the augmented (aug-cc-pV*n*Z) basis sets. Circles denote MP2, squares MP4, and triangles CCSD(T) levels of theory, respectively.

barrier (28.9 cm^{-1}) than that of using the cc-pVTZ vs the cc-pVQZ geometries (0.2 cm^{-1}). This suggests that the optimal geometries are well-converged with the cc-pVTZ basis set and it is more important to carry out single point energy calculations at these geometries rather than reoptimizing the geometry with larger sets. This has also been recently found for the binding energies of small water clusters.[25] Furthermore, it is consistent with the conclusions reached in section III.a regarding the convergence of the optimal geometry with basis set.

The bold entries in Table 3 denote the best estimate for the puckering barrier at the corresponding level of theory and basis set. The results of Table 3 suggest that the basis set dependence at the HF level is quite weak; the range of barrier heights spanned with all basis sets used in this study is just $\sim$6 cm^{-1}. Our results indicate that HF underestimates the puckering barrier by $\sim$150 cm^{-1}, in agreement with previous studies at this level of theory with much smaller basis sets.[16] On the other hand, MP2 produced barrier heights that are too high by 200−330 cm^{-1} with respect to the range of values determined experimentally. The effect of basis set at the MP2 level of theory is to reduce the barrier, but even the largest aug-cc-pV5Z set produces a value that is $\sim$200 cm^{-1} larger than the range of experimental estimates. The largest incremental decrease (87 cm^{-1}) with basis set size occurs between the values computed with the cc-pVTZ and cc-pVQZ sets. Similar trends were observed for the augmented sets (aug-cc-pV*n*Z, n = D, T, Q) for which a decrease of 120 cm^{-1} in the barrier is observed between the values computed with the aug-cc-pVDZ and aug-cc-pVTZ sets. This finding, as well as the results of Table 3, suggests a faster convergence of the barrier height with the augmented rather than with the plain correlation-consistent sets. Typically it is found that the aug-cc-pV*n*Z sets produce barrier heights that are of comparable magnitude to the ones produced with the cc-pV(n+1)Z sets. A recent study by Glendening and Halpern[26] reported the calculation of the ring puckering barrier at the B3LYP, MP2, and CCSD(T) levels of theory with just the plain (cc-pV*n*Z, n = D, T, Q) basis sets. Their results are similar with the ones shown in Figure 2 with the same (nonaugmented) basis sets: they correspond to a curve that is concave downward (up to the QZ set) with the cardinal basis set index n and therefore quite difficult to extrapolate to the CBS limit. In contrast, the use of the aug-cc-pV*n*Z sets (cf. Figure 2) results in a curve that is concave upward with n and easier to extrapolate to the CBS limit. In any event, our results with the larger basis set of 5Z quality reported here make the CBS extrapolation process more accurate.

The CBS limit for the barrier height at the MP2 level is estimated at 691 cm^{-1} with the plain (except for cc-pVDZ) and 687.3 ± 0.3 cm^{-1} with the augmented families of basis sets following the previously proposed heuristic extrapolation scheme that is based on an exponential[27] variation of the barrier height with the cardinal number of the basis set n. It should be emphasized that the extrapolation procedure lowers the best-calculated number at the MP2 level of theory (696 cm^{-1} with the aug-cc-pV5Z set) by just 9 cm^{-1}. The MP2/CBS limit therefore overestimates the experimentally determined barrier height by at least 175 cm^{-1}.

Increasing the level of electron correlation results in the lowering of the barrier, as evident from the MP4(SDTQ) and CCSD(T) results of Table 3 and the traces in Figure 2. The lowering of the barrier for these methods with respect to MP2 is exclusively an effect of the inclusion of higher correlation (triple excitations), not one attributed to the possibility that the geometries are not converged at the MP2 level. This is supported by the fact that a single point MP2/aug-cc-pVTZ calculation at the CCSD(T)/aug-cc-pVTZ optimal geometries for the two stationary points produces a barrier of 743 cm^{-1}, very close to the corresponding value of 756 cm^{-1} at the MP2/aug-cc-pVTZ optimal geometries (cf. Table 2). As in the case of MP2, the larger incremental drop in the computed barrier with basis set occurs between cc-pVTZ/cc-pVQZ for the plain sets [95.6 cm^{-1} for both CCSD(T) and MP4] and aug-cc-pVDZ/aug-cc-pVTZ for the augmented ones [129 cm^{-1} for CCSD(T) and 129.7 cm^{-1} for MP4]. In fact, the incremental variation of the barrier height with basis set is almost identical (within < 1 cm^{-1}) between CCSD(T) and MP4 with both families of basis sets. This is readily seen from Figure 2, where the traces of the CCSD(T) and MP4 results are parallel to each other.

TABLE 4: Shifts in the Barrier Heights: $\Delta\Delta E$ (MP2-λ; n) and $\delta\Delta\Delta E$ (n + 1; n)[a]

level of theory λ	basis set n	geometry	$\Delta\Delta E$ (MP2-λ; n), cm^{-1}	$\delta\Delta\Delta E$ (n + 1; n), cm^{-1}
CCSD(T)	cc-pVDZ	optimized	172.1	
	cc-pVTZ	optimized	180.7	8.6
	cc-pVQZ	cc-pVTZ	188.8	8.1
	cc-pV5Z	cc-pVTZ	188.3	−0.5
	aug-cc-pVDZ	optimized	183.4	
	aug-cc-pVTZ	optimized	191.8	8.4
	aug-cc-pVQZ	aug-cc-pVTZ	191.6	−0.2
MP4	cc-pVDZ	optimized	129.5	
	cc-pVTZ	optimized	139.0	9.5
	cc-pVQZ	cc-pVTZ	148.1	9.1
	aug-cc-pVDZ	optimized	141.8	
	aug-cc-pVTZ	optimized	150.8	9.0
	aug-cc-pVQZ	aug-cc-pVTZ	151.0	0.2

[a] $\Delta\Delta E$ (MP2-λ; n) is the difference between the barrier height at level of theory λ [CCSD(T), MP4] and the corresponding MP2 value; geometries at levels of theory λ and MP2 optimized with the same basis set are used as references. $\delta\Delta\Delta E$ (n + 1; n) is the incremental change of the previous quantity with basis set at a fixed level of theory.

To arrive at the CBS estimates of the barrier height for the higher correlation methods [MP4, CCSD(T)], we used the following two procedures: (a) extrapolation assuming an exponential functional of the CCSD(T) and MP4 results and (b) estimates based on the difference between CCSD(T) and/or MP4 from the MP2 results.

The first approach can be used if results with the larger basis sets are available, as in the present case. However, especially for the per-substituted species such as C_4F_8 and $C_4(OH)_8$, calculations with the largest sets may be currently feasible for MP2 but not with higher correlation methods such as CCSD-(T) and MP4. In this case, the MP2 results can be used as guidance in order to arrive at more accurate estimates for the barrier height with those higher correlation methods. The difference

$$\Delta\Delta E\ (\text{MP2-}\lambda;\ n) = \Delta E\ (\text{MP2};\ n) - \Delta E\ (\lambda;\ n) \qquad (1)$$

between the barrier height at level of theory λ = CCSD(T), MP4, and the corresponding MP2 result with the same basis set n is shown in Table 4. Here the reference geometries are optimized at levels of theory λ [CCSD(T), MP4] and MP2 with the same basis set, respectively. This difference increases with basis set n, but its incremental change with basis set

$$\delta\Delta\Delta E\ (n+1;\ n) = \Delta\Delta E\ (\text{MP2-}\lambda;\ n+1) - \Delta\Delta E\ (\text{MP2-}\lambda;\ n) \qquad (2)$$

TABLE 5: Normal Modes for Cyclobutane (C_4H_8) Minimum (D_{2d} Symmetry)[a]

symmetry	harmonic (cm^{-1})	IR intensity (km/mol)	IR activity	anharmonic (cm^{-1})	band origin[b] (cm^{-1})	mode description
A_1	3144	0.0	forbidden	2996	2962	CH_2 asym stretch
	3154	0.0		3014		
	3091	0.0		2966	2905	CH_2 sym stretch
	3103	0.0		2993		
	1516	0.0		1490	1469	scissors
	1533	0.0		1480		
	1169	0.0		1141	1153	rock
	1182	0.0		1154		
	1038	0.0		1014	1005	ring stretch (breathing)
	1044	0.0		1020		
	249	0.0		235	199	ring puckering
	250	0.0		235		
A_2	1235	0.0	forbidden	1210	1258	wag + twist
	1258	0.0		1230		
	951	0.0		940	943	twist + wag
	965	0.0		953		
B_1	1248	0.0	forbidden	1216	1234	twist + wag + ring stretch
	1262	0.0		1231		
	1153	0.0		1121	1139	wag + twist
	1170	0.0		1138		
	950	0.0		928	926	ring stretch
	957	0.0		935		
B_2	3170	79.7	allowed	3021	2987	CH_2 asym. stretch
	3180	67.0	C-type	3039		
	3085	16.4		2962	2915	CH_2 sym. stretch
	3099	13.8		2991		
	1480	4.7		1440	1454	scissors
	1501	5.5		1460		
	911	0.05		888	892	ring bend + rock
	919	0.04		896		
	617	1.7		619	626	rock + ring bend
	620	2.1		621		
E	3156	25.5	allowed	3007	2968	CH_2 asym. stretch
	3166	22.4		3025		
	3087	65.6	A, B-type	2963	2880	CH_2 sym. stretch
	3100	57.9		2990		
	1471	0.5		1433	1452	scissors
	1492	0.8		1453		
	1270	1.5		1240	1260	twist + wag + ring stretch
	1288	2.2		1256		
	1244	0.4		1212	1224	wag + twist + ring stretch
	1262	0.4		1229		
	921	2.4		902	901	ring stretch
	931	2.9		912		
	753	0.3		747	749	rock + twist
	765	0.4		756		

[a] The calculated harmonic and anharmonic frequencies are obtained at the MP2 level of theory with the aug-cc-pVDZ (first line) and cc-pVTZ (second line) basis sets. [b] From ref 28.

is saturated with the cc-pVQZ and aug-cc-pVTZ sets, respectively, as evident from Table 3.

The exponential extrapolation of the CCSD(T)/cc-pV*n*Z (except for cc-pVDZ) results (method a) yields a barrier of 505 cm^{-1}, while by subtracting a $\Delta\Delta E$ [CCSD(T)-MP2] value of 188 cm^{-1} (Table 3) from the corresponding MP2(cc-pV*n*Z)/CBS value of 691 cm^{-1} (method b) produces a CCSD(T)(cc-pV*n*Z)/CBS estimate of 503 cm^{-1}, just 2 cm^{-1} away from the one obtained with method a. Similarly, the extrapolation of the aug-cc-pV*n*Z results yields CCSD(T)(aug-cc-pV*n*Z)/CBS estimates of 498 cm^{-1} (method a) and 495 cm^{-1} (method b).

As regards the MP4/aug-cc-pV*n*Z results, the exponential extrapolation produces CBS estimates of 538 cm^{-1} (method a), whereas method b yields 536 cm^{-1} [687 cm^{-1} (MP2/CBS) − 151 cm^{-1}). Finally, method b yields 543 cm^{-1} for the cc-pV*n*Z sets at the MP4 level. We note again that the estimates for the barrier obtained with the two methods (a or b) are within <7 cm^{-1} from each other.

From the previous analysis we conclude that our best CBS estimates for the barrier height (obtained with method "a") are 687 cm^{-1} (MP2), 538 cm^{-1} (MP4), and 498 cm^{-1} [CCSD(T)]. The CCSD(T) and MP4 CBS estimates are within 20 cm^{-1} (∼4%) from the best computed values (with the largest basis sets) at these two levels of theory, respectively.

c. Anharmonic Vibrational Spectra. The calculated harmonic and anharmonic vibrational frequencies of cyclobutane at its minimum (D_{2d}) geometry are listed in Table 5 together with the experimentally observed[24,28] band origins. The calculated harmonic and anharmonic frequencies are obtained at the MP2 level of theory with the aug-cc-pVDZ (first line of each entry) and cc-PVTZ (second line of each entry) basis sets. Their infrared (IR) intensities (km/mol), IR activity, as well as the mode description are also indicated. Most of the computed anharmonic frequencies are within 1% from the experimentally observed band origins except for the CH_2 symmetric stretch vibrations of A_1 (2905 cm^{-1}), B_2 (2915 cm^{-1}), and E (2880

cm^{-1}) symmetries, for which the discrepancy is ~3%. Overall, the effect of anharmonicity amounts to a correction of ~330 cm^{-1} (0.95 kcal/mol) to the zero-point energy of the system (cf. Table 2).

IV. Conclusions

In this study we present the results of high-level ab intio calculations for the structure, anharmonic frequencies, and ring-puckering barrier of cyclobutane. In particular, we have taken into account the effects of the level of electron correlation, the orbital basis set, as well as the use of converged geometries in establishing accurate energy differences between the minimum (D_{2d}) and transition state (D_{4h}) configurations.

Our results indicate that the geometry of the minimum is converged with triple-ζ quality basis sets. The computed structures were in good agreement with earlier experimental results obtained using electron diffraction. The difference between the two sets of C−H bond lengths was found to be ~0.002 Å, i.e., below the detection limit of the electron diffraction experiments. Furthermore, we obtained 29.68° for the puckering angle, a value that can be utilized in future analysis of the experimental data.

With regard to the puckering barrier, we followed a systematic procedure in order to arrive at accurate CBS estimates for this quantity. Our results indicate that the HF level of theory underestimates it by ~150 cm^{-1}, whereas MP2 overestimates it by at least 180 cm^{-1}. Higher correlation methods such as MP4 and especially CCSD(T) are needed in order to establish accurate energetics. Even at these higher levels of electron correlation, the basis set effect was found to be significant: basis sets of quadruple-ζ quality or larger are needed in order to produce energy differences that are within 10% or less from the CBS estimates of these methods, which were established at 538 cm^{-1} (MP4) and 498 cm^{-1} [CCSD(T)]. For systems for which these calculations are not currently feasible, we have suggested a procedure for obtaining estimates of the barrier height based on a combination of the results of the cheaper MP2 calculations and the more expensive ones at the CCSD(T) level of theory with smaller basis sets. We will apply this procedure in subsequent studies of higher substituted analogues of cyclobutane such as C_4Cl_8, $C_4(OH)_8$, and C_4F_8.

Finally, we note that our CCSD(T)/CBS estimate of 498 cm^{-1} for the barrier height is in excellent agreement with the one originally suggested by Stone and Mills[6] (503 cm^{-1}). It lies within 10 cm^{-1} from the value obtained in the earlier work of Egawa et al.[9] (510 ± 3 cm^{-1}), which also yielded a value of 28.8 ± 1.1° for the ring-puckering angle, in agreement with our estimate of 29.7°. It is, however, in disagreement with the later work by Egawa et al.,[13] which produced barriers of 649 ± 11 cm^{-1} (one-dimensional treatment with resulting puckering angle of 31.4°) and 449 ± 9 cm^{-1} (two-dimensional treatment with resulting puckering angle of 27.8 ± 1.2°), suggesting that a new analysis of the experimental data might be in order.

Acknowledgment. Part of this work was performed in the William R. Wiley Environmental Molecular Sciences Laboratory (EMSL) under the auspices of the Division of Chemical Sciences, Office of Basic Energy Sciences, US Department of Energy under Contract DE-AC06-76RLO 1830 with Battelle Memorial Institute, which operates the Pacific Northwest National Laboratory. This research was performed in part using the Molecular Science Computing Facility (MSCF) in EMSL, a national user facility funded by the Office of Biological and Environmental Research of the U.S. Department of Energy. Additional computer resources at the National Energy Research Scientific Computer Center (NERSC) were provided by the Division of Chemical Sciences, US Department of Energy.

References and Notes

(1) Lafferty, W. J. *Critical Evaluation of Chemical Physical Structure Information, Proceedings of a Conference*; National Academy of Sciences: Washington, DC, 1974; pp 386-409.

(2) Blackwell, C. S.; Lord, R. C. *Vibrational Spectra and Structure*; Durig, J. R., Ed.; Marcel Dekker: New York, 1972; Vol. 1, Chapter 1.

(3) Chan, S. I.; Zinn, J.; Fernandez, J.; Gwinn, W. D. *J. Chem. Phys.* **1960**, *33*, 1643−1655; *J. Chem. Phys.* **1961**, *34*, 1319−1329. Chan, S. I.; Borgers, T. R.; Russell, J. W.; Straus, H. L.; Gwinn, W. D. *J. Chem. Phys.* **1966**, *44*, 1103−1111. Harris, D. O.; Harrington, H. W.; Luntz, A. C.; Gwinn, W. D. *J. Chem. Phys.* **1966**, *44*, 3467−3480.

(4) Bell, R. P. *Proc. R. Soc. (London)* **1945**, *A183*, 328−337.

(5) Ueda, T.; Simanouchi, T. *J. Chem. Phys.* **1968**, *49*, 470−471.

(6) Stone, J. M. R.; Mills, I. M. *Mol. Phys.* **1970**, *18*, 631−652.

(7) Miller, F. A.; Capwell, R. J. *Spectrochim. Acta* **1971**, *27A*, 947−956. Miller, F. A.; Capwell, R. J. *Spectrochim. Acta* **1972**, 28A, 603−618.

(8) Malloy, T. B., Jr.; Lafferty, W. J. *J. Mol. Spectrosc.* **1975**, *54*, 20−38.

(9) Egawa, T.; Fukuyama, T.; Yamamoto, S.; Takabayashi, F.; Kambara, H.; Ueda, T.; Kuchitsu, K. *J. Chem. Phys.* **1987**, *86*, 6018−6026.

(10) Gordy, W.; Cook, R. L. *Microwave Molecular Spectra*; Wiley-Interscience: New York, 1984.

(11) Bartell, L. S. *J. Chem. Phys.* **1955**, *23*, 1219−1222. Bartell, L. S. *J. Chem. Phys*. **1963** *38*, 1827−1833.

(12) Cremer, D. *J. Am. Chem. Soc.* **1977**, *99*, 1307−1309.

(13) Egawa, T.; Yamamoto, S.; Ueda, T.; Kuchitsu, K. *J. Mol. Spectrosc*. **1987**, *126*, 231−239.

(14) Champion, R.; Godfrey, P. D.; Bettens, F. L. *J. Mol. Spectrosc.* **1992**, *155*, 18−24.

(15) Fischer, G.; Purchase, R. L.; Smith, D. M. *J. Mol. Struct.* **1997**, *405*, 159−167.

(16) Henseler, D.; Hohlneicher, G. *J. Phys. Chem. A* **1988**, *102*, 10828−10833.

(17) Dunning, T. H., Jr. *J. Chem. Phys*. **1989**, *90*, 1007−1023. Kendall, R. A.; Dunning, T. H., Jr.; Harrison, R. J. *J. Chem. Phys*. **1992**, *96*, 6796−6806.

(18) Clabo, D. A., Jr.; Allen, W. D.; Remington, R. B.; Yamaguchi, Y.; Schaefer, H. F., III. *Chem. Phys*. **1988**, *123*, 187−239. Allen, W. D.; Yamaguchi, Y.; Császár, A. G.; Clabo, D. A., Jr.; Remington, R. B.; Schaefer, H. F., III. *Chem. Phys*. **1990**, *145*, 427−466. Miller, W. H.; Hernandez, R.; Handy, N. C.; Jayatilaka, D.; Willets, A. *Chem. Phys. Lett*. **1990**, *172*, 62−68; Barone, V. *J. Chem. Phys*. **2004**, *120*, 3059−3065. Barone, V. *J. Chem. Phys*. **2005**, *122*, 014108.

(19) Barone, V. *J. Chem. Phys*. **1994**, 101, 10666−10676. Minichino, C.; Barone, V. *J. Chem. Phys*. **1994**, *100*, 3717−3741. Barone, V.; Minichino, C. *THEOCHEM* **1995**, *330*, 365−376.

(20) Frisch, M. J.; et al. *Gaussian 98*, Revision A.9; Gaussian Inc.: Pittsburgh, PA 1998. Frisch, M. J.; et al. *Gaussian 03*, Revision C.02; Gaussian Inc.: Wallingford, CT 2004.

(21) MOLPRO is a package of ab initio programs written by Werner, H.-J.; Knowles, P. J., with contributions from Amos, R. D.; Bernhardsson, A.; Berning, A.; Celani, P.; Cooper, D. L.; Deegan, M. J. O.; Dobbyn, A. J.; Eckert, F.; Hampel, C.; Hetzer, G.; Korona, T.; Lindh, R.; Lloyd, A. W.; McNicholas, S. J.; Manby, F. R.; Meyer, W.; Mura, M. E.; Nicklass, A.; Palmieri, P.; Pitzer, R.; Rauhut, G.; Schütz, M.; Stoll, H.; Stone, A. J.; Tarroni, R.; Thorsteinsson, T.

(22) Anchell, J.; et al. "*NWChem, A Computational Chemistry Package for Parallel Computers*, Version 4.0"; Pacific Northwest National Laboratory: Richland, WA 99352-0999, 1999.

(23) Wilson, E. B., Jr.; Decius, J. C.; Cross, P. C. *Molecular Vibrations*; Dover Publications: New York, 1980.

(24) Li, H.; Miller, C. C.; Philips, L. A. *J. Chem. Phys.* **1994**, *100*, 8590−8601.

(25) Xantheas, S. S.; Burnham, C. J.; Harrison, R. J. *J. Chem. Phys.* **2002**, *116*, 1493−1499.

(26) Glendening, E. D.; Halpern, A. M. *J. Phys. Chem. A* **2005**, *109*, 635−642.

(27) Feller, D. *J. Chem. Phys.* **1992**, *96*, 6104−6114. Xantheas, S. S.; Dunning, T. H., Jr. *J. Phys. Chem.* **1993**, *97*, 18−19. Xantheas, S. S.; Dunning, T. H., Jr. *J. Phys. Chem.* **1993**, *97*, 6616−6627.

(28) Annamalai, A.; Keiderling, T. A. *J. Mol. Spectrosc*. **1985**, *109*, 46−59.